J. Membrane Biol. 193, 23–34 (2003)
DOI: 10.1007/s00232-002-2004-6

The Journal of
Membrane
Biology

© Springer-Verlag New York Inc. 2003

Gating Properties of a Sodium Channel with Three Arginines Substituted by Histidines in the Central Part of Voltage Sensor S4D4

F.J.P. Kühn, N.G. Greeff
Physiologisches Institut, Universität Zürich, Winterthurerstr. 190, CH-8057 Zürich, Switzerland

Received: 2 October 2002/Revised: 21 January 2003

Abstract. In voltage-dependent sodium channels there is some functional specialization of the four different S4 voltage sensors with regard to the gating process. Whereas the voltage sensors of domains 1 to 3 control activation gating, the movement of the voltage sensor of domain 4 (S4D4) is known to be tightly coupled to sodium channel inactivation, and there is some experimental evidence that S4D4 also participates in activation gating. To further explore its putative multifunctional role in the gating process, we changed the central part of S4D4 in rat brain IIA (rBIIA) sodium channels by the simultaneous replacement of the third (R1632), fourth (R1635) and fifth (R1638) arginine by histidine (mutation R3/4/5H). As a result, the time course of current decay observed in R3/4/5H was about three times slower, if compared to wild type (WT). On the other hand, the recovery, as well as the voltage dependence of fast inactivation, remained largely unaffected by the mutation. This suggests that at physiological pH (7.5) the effective charge of the voltage sensor was not significantly changed by the amino-acid substitutions. The well-known impact of site-3 toxin (ATX-II) on the inactivation was drastically reduced in R3/4/5H, without changing the toxin affinity of the channel. The activation kinetics of WT and R3/4/5H studied at low temperature (8°C) were indistinguishable, while the inactivation time course of R3/4/5H was then clearly more slowed than in WT. These data suggest that the replacement of arginines by histidines in the central part of S4D4 clearly affects the movement of S4D4 without changing the activation kinetics.

Correspondence to: N.G. Greeff; email: greeff@physiol.unizh.ch

Abbreviations: rBIIA, rat brain IIA; TEVC, two-electrode voltage clamp; R_s, series resistance; TTX, tetrodotoxin; I_{Na}, sodium current; MTSET, 2-trimethylammonium-ethyl-methanethiosulfonate; ATX-II, sea anemone toxin.

Key words: Voltage sensor S4D4 — Mutagenesis — ATX-II — Fast inactivation — Activation

Introduction

Voltage-dependent sodium channels are characterized by four distinct positively charged transmembrane segments that serve as sensors for changes of the membrane potential (Catterall, 1986; Noda et al., 1986; Stühmer et al., 1989; Yang and Horn, 1995). Besides, there are two kinetically defined types of gates for the control of channel activation and fast inactivation, respectively (Sigworth, 1993; Yellen, 1998). However, the choreography of interactions between voltage sensors and gates necessary for the opening and closure of the channel pore until now is poorly understood. The systematic analysis of sodium channels containing point mutations in either of the four S4 segments reveals that in particular the voltage sensor of domain 4 (S4D4) is involved in fast inactivation gating, whereas the S4-segments of domains 1–3 are mainly coupled to the activation process (Chahine et al., 1994; Chen et al., 1996; Kontis & Goldin, 1997; Kontis, Rounaghi & Goldin, 1997; Cha et al., 1999; Kühn & Greeff, 1999). In a previous study we proposed a model where S4D4 moves in two separate steps with an initial step or delay perhaps involved in activation and a second step that controls fast inactivation (Kühn & Greeff, 1999). In line with this hypothesis are the recent findings of Horn, Shinghua and Gruber (2000), which indicate that the movement of S4D4 is a two-step process, each step coupled to a different gate. On the other hand, the data of Sheets and Hanck (1995), Sheets et al. (1999) and Sheets, Kyle and Hanck (2000) suggest that the movement of S4D4 is selectively inhibited in the presence of site-3 toxins. As a result, the available gating charge was reduced by about one third and

sodium channel fast inactivation kinetics was drastically changed. However, corresponding effects on activation gating were not noticed by these authors.

To further elucidate the putative role of S4D4 in sodium channel gating, we continued our earlier strategy to disturb the mobility of this voltage sensor by the replacement of arginines by histidines. In addition to the substitutions used so far, R1635H and R1638H and the double mutation R1635H/R1638H (*see* Kühn & Greeff, 1999), we added R1632H and could successfully express the triple mutation. Thereby, we extended the histidine modification further towards the narrow pore that is regarded to represent that part of the channel protein where the actual voltage drop and voltage sensing occur (Yang, George & Horn, 1996). In this way, we wanted to inhibit further or freeze the movement of S4D4. Of special interest was also to inquire whether in addition to the slowing of inactivation we would now observe a slowing or stop of activation, i.e., to search for evidence of an involvement of S4D4 in activation. Experiments were carried out also at low temperature for better temporal resolution and furthermore, we analyzed the impact of the known modifier of S4D4 mobility, the site-3 toxin ATX-II, on channel gating. The results strongly support earlier findings that the mobility of S4D4 determines the fast inactivation kinetics while we still found no convincing evidence for an involvement of this voltage sensor in activation gating.

Materials and Methods

Mutagenesis and Expression of Channels

The cDNAs of both the wild-type rat brain IIA (rBIIA) sodium channel α subunit and the β_1 subunit used in this study were derived from plasmid pVA2580 and pBluescript SK$^-$, respectively, and transferred into high-expression vector pBSTA. The resulting plasmids pBSTA(α) and pBSTA(β) contain a T7 RNA polymerase promotor and *Xenopus*-β-globin 5′ and 3′ untranslated sequences that greatly increase the expression of exogenous proteins in oocytes (Shih et al., 1998). Site-directed mutagenesis was performed as previously described (Kühn & Greeff, 1999). The presence of inadvertent mutations in other regions of the channel could be excluded because several mutant clones tested yielded the same results. In addition, the mutations were verified by DNA sequencing. Capped, full-length transcripts were generated from *SacII* linearized plasmid DNA using T7 RNA polymerase (mMessage mMachine In Vitro Transcription Kit from Ambion, Austin, TX). Large oocytes (stage V–VI; 1.2 mm diameter on average) from *Xenopus laevis* (NASCO, Ft. Atkinson, WI) were used. For surgical removal of the oocytes, female frogs were anaesthetized with 0.15% tricaine (3-aminobenzoic acid ethyl ester; Sigma, St. Louis, MO) and placed on ice. Frogs were allowed to recover at least 6 months following surgery. All animal handling was carried out in accordance with methods approved by Swiss Government authorities.

One day before injection of complementary RNA (cRNA), the oocytes were defolliculated in a Ca^{2+}-free solution containing 2 mg/ml collagenase (Boehringer, Mannheim, Germany), for ~2 h at room temperature. Oocytes were microinjected with 50 ng cRNA of WT or mutant α-subunit and—if coexpression was needed—100 ng of β-subunit in a 1:1 volume of 50 to 100 nl, and maintained at 18 ± 1°C in Modified Barth's Solution (MBS, in mM) 88 NaCl, 2.4 $NaHCO_3$, 1 KCl, 0.82 $MgSO_4$, 0.41 $CaCl_2$ 0.33 $Ca(NO_3)_2$, 10 HEPES-CsOH, pH 7.5, supplemented with 25 U penicillin, 25 μg/ml streptomycin-sulfate and 50 μg/ml gentamycin-sulfate. For the partial reduction of the large WT ionic current, TTX (RBI-Research Biochemicals International, Natick, MA) was added to the recording chamber. Sea anemone toxin (ATX-II) from *Anemonia sulcata* (Sigma) was used in concentrations between 0.13 μM and 2 μM. Allowance for distribution of ATX-II in the bath and towards the oocyte membrane of 5 minutes was found sufficient, since no further increase of the effect was observed after 10 and 15 minutes.

Electrophysiology and Data Acquisition

Two-electrode voltage-clamp recordings were performed 2 to 6 days after cRNA-injection with a TEC-05 (npi-electronic, Tamm, Germany) that had been modified for improved compensation of the series resistance (R_s) and for fast charging of the membrane capacitance (Greeff & Polder, 1998; Greeff & Kühn, 2000). Intracellular agarose cushion electrodes (Schreibmayer, Lester & Dascal, 1994) were filled with 3 M KCl and had a resistance between 50 and 150 kΩ. Macroscopic I_{Na} and I_g signals were recorded using a PDP-11/73 computer (Digital Equipment, Maynard, MA) controlling a 16-bit A/D and 12-bit D/A interface (CED, Cambridge, UK). The oocytes were clamped at a holding potential of −100 mV for at least 5 minutes to ensure recovery from slow inactivation before recording started. The experiments were done at temperatures of +15 or +8 ± 1°C controlled by a Peltier element. R_s compensation was adjusted critically to accelerate the settling time of the capacitance transients within 200 μs (without low pass filtering, *see* below). No analog subtraction was used, since the 16-bit ADC had a sufficiently fine resolution for digital subtraction of the linear transient and leak currents by scaled averages from pulses between −120 mV and −150 mV. Reduction of the remaining asymmetry was achieved by finding a compromise between clamping speed and asymmetry, i.e., by low-pass-filtering the command signal at 5 kHz (8-pole Bessel). Signals were low-pass filtered at 5 kHz (−3 dB) and sampled at 10 or 20 kHz. The actual clamp speed at the oocyte membrane was determined from the integrated capacitance transient to have a time constant between 150 to 200 μs. R_s errors were <5 mV unless the currents exceeded ~20–30 μA. Data analysis was performed on the PDP-11 and additionally with the Windows-compatible programs UN-SCAN-IT™ (Silk Scientific, Orem, UT) and PRISM™ (GraphPad Software, San Diego, CA).

Results

Expression and Voltage-dependent Gating

Figure 1*A* shows the macroscopic sodium currents of WT and triple mutant R1632H/R1635H/R1638H (subsequently denoted as R3/4/5H, since third to fifth arginines of voltage sensor S4D4 were changed to histidines). Despite of using a high-expression system, (*see* Methods) that usually produces sodium currents of 50–100 μA and gating currents of 5–10 μA for WT and other S4D4 mutants in our lab (Kühn & Greeff, 1999), the mutant R3/4/5H consistently showed a decreased expression level (maximum I_{Na} of 3–4 μA)

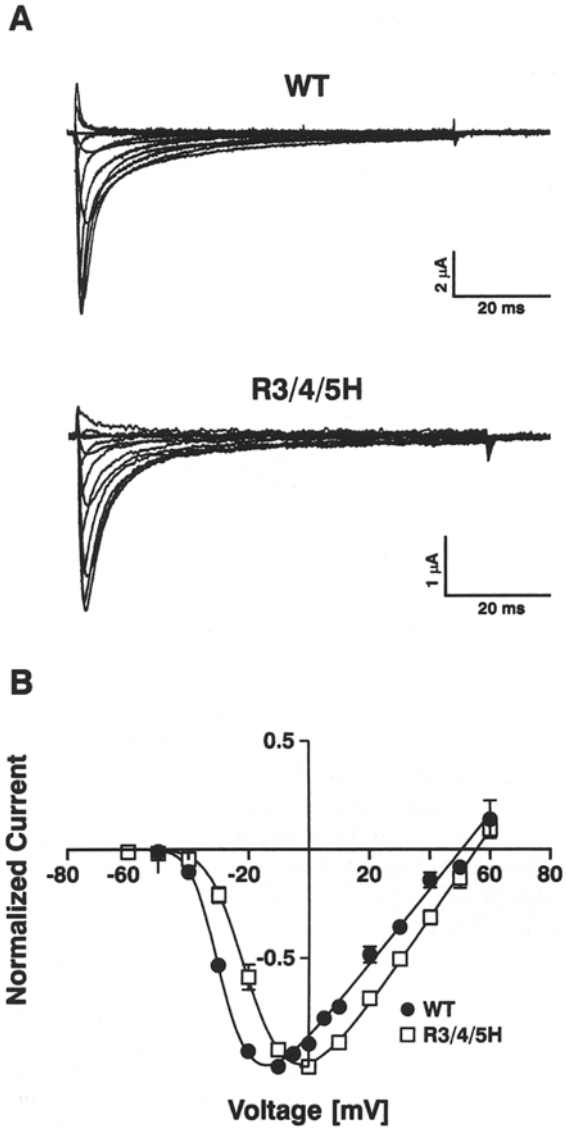

Fig. 1. Expression level and macroscopic Na^+ currents. (*A*) Na^+ currents from WT- and R3/4/5H- injected *Xenopus* oocytes were elicited by step-depolarizations of −80 mV to +80 mV, from a holding potential of −100 mV. In order to minimize possible R_s-distortions, the large WT sodium currents were reduced to 5–10 µA by application of TTX. The mutant R3/4/5H produces only sodium currents smaller than 4 µA and hence currents were not significantly disturbed by R_s. (*B*) Corresponding current-voltage relationship of peak Na^+ currents, normalized to the largest inward current. The data (mean ± SEM of $n = 3$ cells) were fitted to the equation $Y = G \cdot (X - V_{Na})/(1 + \exp((V_M - X)/k_V))^3$ where V_{Na} is the reversal potential of Na^+, V_M is the half-activation potential and k_V, a slope factor. For WT, V_{Na} = 50.6 ± 1.2 mV, V_M = −36.9 ± 0.7 mV and k_V = 7.04 ± 0.7 mV and for R3/4/5H, V_{Na} = 55.6 ± 0.8 mV, V_M = −29.6 ± 0.6 mV and k_V = 9.6 ± 0.6 mV.

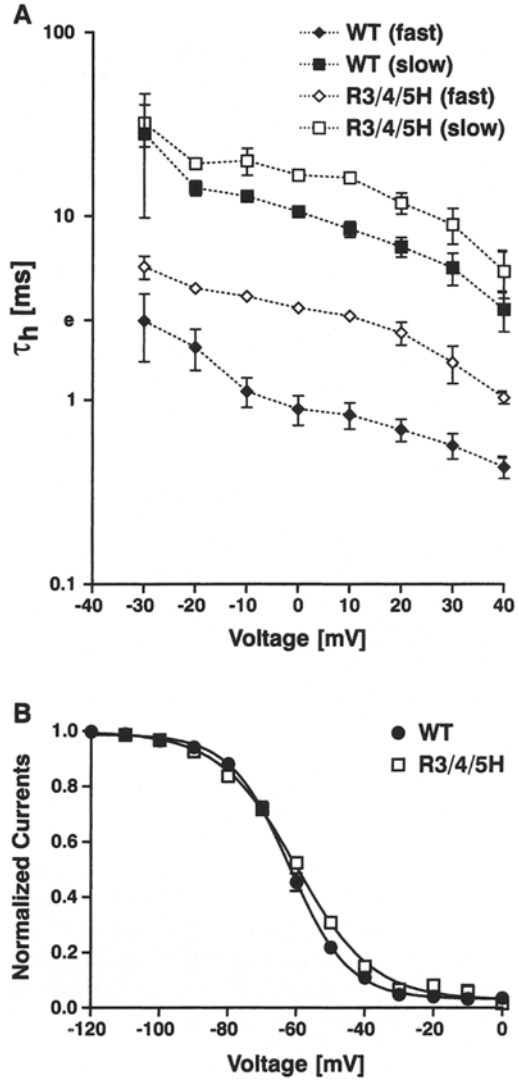

Fig. 2. Voltage independence of fast inactivation. (*A*) Semilogarithmic plot of the voltage dependence of the inactivation time constants, $\tau_{h(fast)}$ and $\tau_{h(slow)}$. The data (mean ± SEM of $n = 4$ cells) were obtained from current traces elicited between −30 and +40 mV from a holding potential of −100 mV (as shown in Fig. 1*A*) and fitted to a double exponential of the form $Y = (1 - \exp(-t/\tau_m))^3 \cdot [A1 \cdot \exp(-t/\tau_{h1}) + A2 \cdot \exp(-t/\tau_{h2}) + A3]$. (*B*) Steady-state inactivation at 0 mV induced by a 100 ms prepulse at voltages between −120 mV and 0 mV in increments of 10 mV at a holding potential of −100 mV. The curves are fitted to a standard Boltzmann distribution of the form $I/I_{max} = 1/(1 + \exp[(V - V_{0.5})/k_V])$. The half-maximal inactivation ($V_{0.5}$) was −62 ± 0.4 mV for WT and −60.2 ± 0.6 mV for R3/4/5H. The slope factor (k_v) of the curve was −8.70 ± 0.4 mV for WT and −11.3 ± 0.5 mV for R3/4/5H. Values are mean ± SEM of $n = 5$ cells.

that was at least one order of magnitude below the corresponding WT level. Likewise, the gating currents of R3/4/5H were too small (≤0.5 µA) to be unequivocally separated from asymmetry artifacts and baseline distortions, respectively. Nevertheless, the corresponding sodium current was large enough for the characterization of the gating kinetics of R3/4/5H.

In order to minimize possible R_s-distortions, the large WT currents were reduced by application of about 100 nM TTX to below 10 µA, as shown in Fig. 1*A*. The scaled current-voltage plots of peak currents

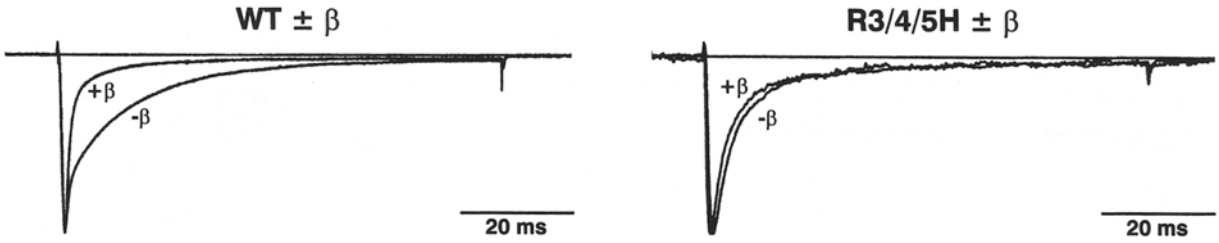

Fig. 3. Bimodal gating and effects of the accessory β_1 subunit on the inactivation kinetics. Typical current traces of WT and R3/4/5H elicited at 0 mV from a holding potential of −100 mV with or without β_1 coexpression; test pulse duration 80 ms. Traces were normalized to peak. Note the pronounced bimodal gating behavior of WT with the drastic shift to the fast gating mode induced by β_1 that is not observed in R3/4/5H. The corresponding inactivation time constants are given for 3 similar experiments each for WT and mutant in the text. Functional differences due to limiting amounts of β_1 subunits in the cells could be excluded because an excess of β_1 cRNA was coinjected.

Table 1. Time constants of I_{Na}-decay of WT and R3/4/5H at different bath temperatures

Voltage	WT (T = 15°C) $\tau_{h\ (fast/slow)}$	WT (T = 8°C) $\tau_{h\ (fast/slow)}$	R3/4/5H (T = 15°C) $\tau_{h\ (fast/slow)}$	R3/4/5H (T = 8°C) $\tau_{h\ (fast/slow)}$
−20 mV	1.94 ± 0.8/14.2 ± 2.3	3.09 ± 0.9/19.5 ± 0.3	4.05 ± 0.4/19.3 ± 2.0	14.3 ± 0.9/212 ± 77
0 mV	0.89 ± 0.3/10.6 ± 1.2	1.92 ± 0.01/15.3 ± 1.8	3.17 ± 0.2/16.7 ± 0.7	10.4 ± 1.1/59 ± 7.6
20 mV	0.69 ± 0.2/6.83 ± 1.4	1.39 ± 0.1/11 ± 0.6	2.32 ± 0.7/11.8 ± 3.2	8.6 ± 0.4/54.1 ± 12.4

The data (mean ± SD of n = 3 cells) were obtained as described in the legend of Fig. 2.

obtained from WT or R3/4/5H and fitted as described in the figure legend suggest a slight depolarizing shift of ~7 mV for the mutant (Fig. 1*B*). This shift might be due to some still uncompensated R_s-distortion, which would shift the I/V-curve of WT to more hyperpolarizing potentials. As discussed in context of Fig. 8, a distortion of peak currents and hence the I/V-curve, is also likely due to changes in inactivation kinetics.

Time Course of Fast Inactivation

The kinetics of current decay was analyzed by performing double-exponential fits from normalized current traces elicited between −30 mV and +40 mV (Fig. 2*A*). In the absence of the β_1-subunit, rat brain IIA (rBIIA) sodium channels show a pronounced bimodal gating if expressed in *Xenopus* oocytes, as already recognized for neuronal and skeletal muscle sodium channels (e.g., Isom et al., 1992; Patton et al., 1994). As described in the context of Fig. 3, we noted that coexpression of the β_1-subunit exerts different effects on the inactivation gating of WT and R3/4/5H and, therefore, we compared the inactivation time courses without β_1 coexpression. The fast gating channels of WT inactivated approximately ten times faster than the corresponding slow-mode channels, which result is in agreement with data obtained from other groups (Moorman et al., 1990; Zhou et al., 1991; Ji et al., 1994; Moran et al., 1998). If compared to WT, the current decay of R3/4/5H also showed a slow and a fast inactivating phase (*see* Fig. 1*A*), as verified by the double-exponential fit (Fig. 2*A*). The fast-mode kinetics determined at 15 °C bath temperature was about three times slower in R3/4/5H than observed in WT, whereas the corresponding time constants of the slow mode were only about 1.5-fold slower in the mutant (Fig. 2*A* and Table 1). For the most significant voltage range between −20 mV and +40 mV, the voltage dependence of fast inactivation of both kinetic populations was determined as an e-fold decrease within 74 mV for WT and 79 mV for R3/4/5H (Fig. 2*A*). Likewise, the voltage dependence of steady-state inactivation was slightly decreased in the mutant, but the midpoint of the curve was almost identical in WT and R3/4/5H (Fig. 2*B*). Therefore, similar to the previously described mutations R4H, R5H and R4/5H (Kühn & Greeff, 1999), the triple mutation R3/4/5H slowed the fast inactivation kinetics and, in addition, moderately decreased the voltage dependence of channel inactivation.

Coexpression of the β_1-Subunit

Hitherto, the effect of the accessory β_1 subunit on the gating kinetics of α subunits expressed in *Xenopus* oocytes were primarily studied in WT sodium channels (for review *see* Isom, De Jongh & Catterall, 1994) and in sodium channels containing mutations that are located outside of the S4 voltage sensors (e.g., Balser et al., 1996; Moran et al., 1998; Kühn & Greeff, 2002). As shown in Fig. 3, the slow gating mode was very prominent in recordings obtained from the WT rBIIA α subunit where β_1 coexpression largely shifts the time course of inactivation to the fast gating

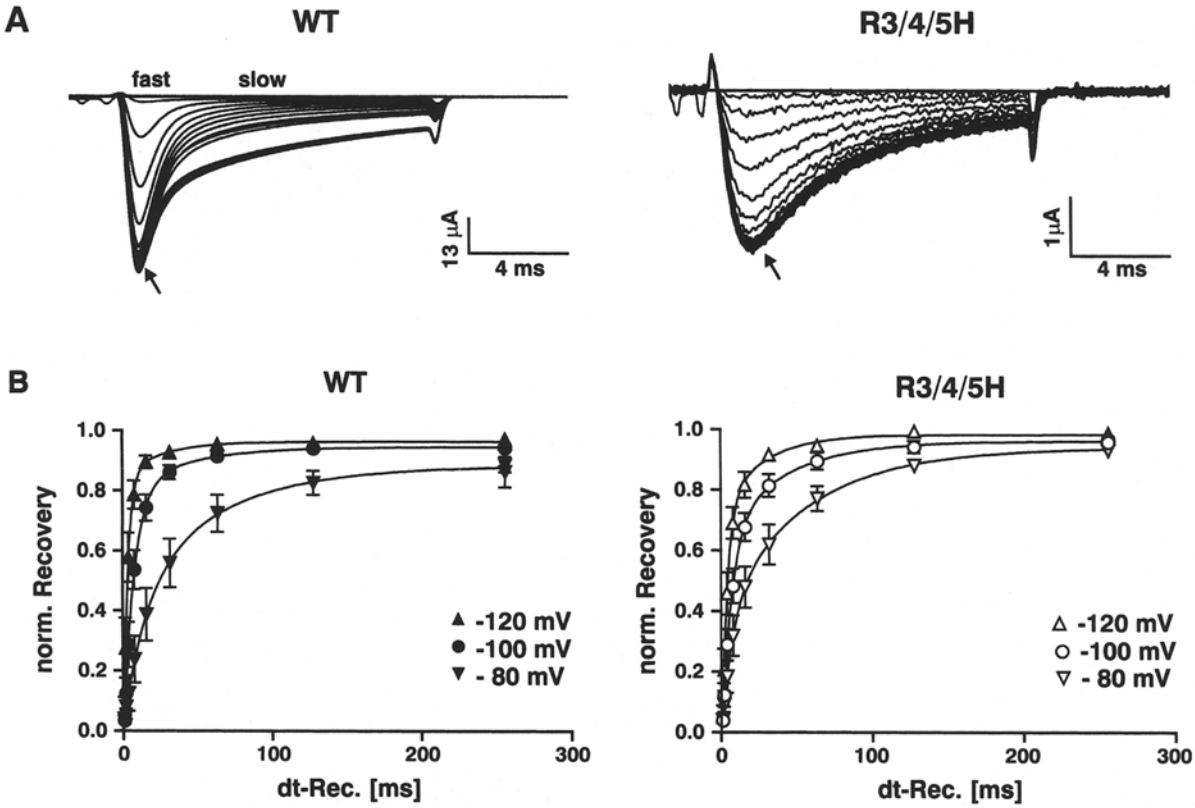

Fig. 4. Recovery from fast inactivation. (*A*) Original recordings of I_{Na} during recovery from fast inactivation of WT and R3/4/5H. The inactivating conditioning pulse to 0 mV from a holding potential of −100 mV had a duration of 100 ms. Interpulse intervals were increased logarithmically from 1 ms to 256 ms at a recovery potential of −100 mV and were followed by a 13-ms test pulse to 0 mV. Responses are superimposed for all recovery periods. Control traces obtained without inactivating prepulse are also included (*arrows*). Note the predominance of the fast or the slow gating mode in WT at different points in the course of the current decay (as indicated). (*B*) Time course of recovery from fast inactivation of WT and R3/4/5H obtained from peak I_{Na} at three different recovery potentials, pulse protocol as described in *A*. For the calculation of the recovery kinetics, the current traces with prepulse were routinely normalized to the current traces without prepulse in order to compensate for the possible decrease due to rundown of the current amplitude in the course of the experiment. For the same reason, the first and the last recovery time interval of the pulse protocol were of identical duration (256 ms). The data (mean ± SEM) were obtained from three (WT) and four (R3/4/5H) single-cell experiments and fitted to a double exponential curve of the form: $Y = A1 \cdot (1 - \exp(-t/\tau_{R1})) + A2 \cdot (1 - \exp(-t/\tau_{R2})) + P$ with corresponding recovery time constants given in the text.

mode (previously described by Bennett, Makita & George, 1993; Patton et al., 1994). Furthermore, the kinetics of both gating modes was slightly accelerated with corresponding time constants ($\tau_{h(fast)}$ / $\tau_{h(slow)}$ in ms; mean ± SEM, n = 3), as derived from similar recordings as shown in Fig. 3, for WT−β: (0.69 ± 0.13 / 14.8 ± 4.6) and for WT + β: (0.69 ± 0.11 / 9.1 ± 1.7)

In contrast, the inactivation time course of R3/4/5H showed visually only little change due to the coexpression of the β_1 subunit, and the slow component was anyway small and hardly changed in magnitude due to the β_1 subunit (Fig. 3). The corresponding time constants ($\tau_{h(fast)}$ / $\tau_{h(slow)}$ in ms; mean ± SEM, n = 3, as dervied from recordings as shown in Fig. 3 were for R3/4/5H−β: (3.8 ± 0.6 / 18.8 ± 1.6) and R3/4/5H + β: (2.24 ± 0.5 / 16.6 ± 6.5). Thus, the impact of the β_1 subunit on the time course of inactivation was significantly less pronounced in R3/4/5H compared to WT.

Recovery from Fast Inactivation

In the absence of β_1 coexpression, the recovery time course of WT was clearly bimodal, with a slow channel population showing incomplete recovery still after an interpulse interval of 256 ms at −100 mV, when the fast mode channels had completely recovered (Fig. 4*A*). In contrast, R3/4/5H did not show such clearly separable recovery kinetics (Fig. 4*A*). This result agrees with the more monophasic inactivation kinetics of R3/4/5H due to the relatively small slowly inactivating population, as described in the context of Figs. 2 and 3. However, the double-exponential fits of the recovery time courses recorded at recovery potentials of −80 mV, −100 mV and −120 mV demonstrate that the recoveries of WT and R3/4/5H were rather similar (Fig. 4*B*), and trials to fit the recovery of the mutant with one exponential only were markedly worse. The corresponding recovery

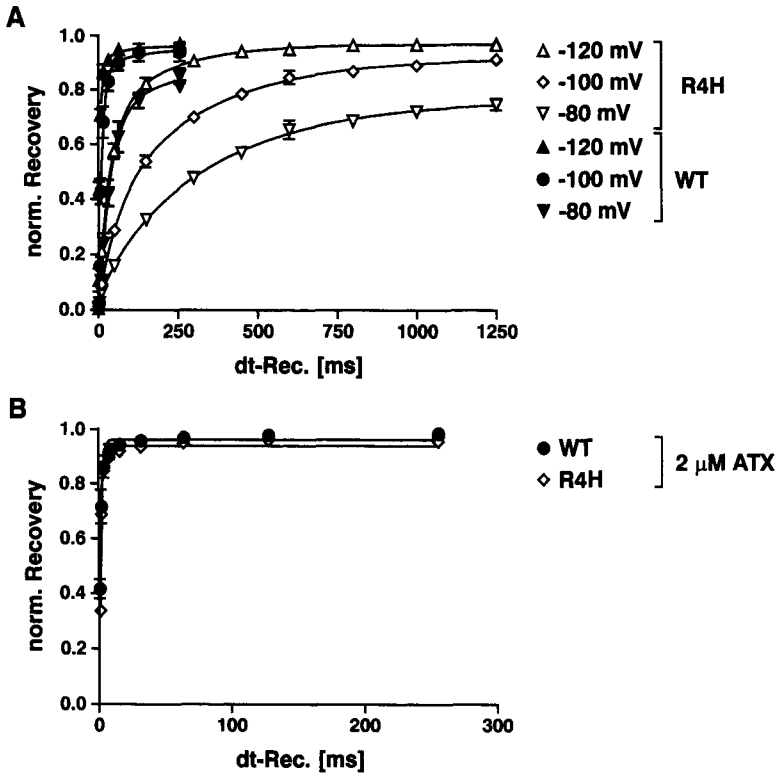

Fig. 5. Recovery kinetics of WT and mutant R1635H in the presence of 2 μM ATX-II. (*A*) Comparison of the recovery time course from fast inactivation of WT and R1635H (R4H) in the absence of ATX-II (*see* also Kühn & Greeff, 1999). Same pulse protocol as described in the legend of Fig. 4, but with regard to the different recovery kinetics of WT and R4H, separate interpulse-intervals were used. The data (mean ± SEM of $n = 2$ cells) were obtained from single-cell experiments at the indicated recovery potentials and fitted as described in the legend of Fig. 4*B* with dominant recovery time constants in ms. WT-α: 38 ± 3.9 (−80 mV), 10.7 ± 4.6 (−100 mV), 4.6 ± 1.1 (−120 mV); R1635H-α: 320 ± 39 (−80 mV), 199 ± 26 (−100 mV), 71 ± 11 (−120 mV). (*B*) Recovery of WT and R4H in the presence of 2 μM ATX-II obtained at a recovery potential of −100 mV. Pulse protocol and fitting of the data as described in the legend of Fig. 4 with dominant recovery time constants in ms (mean ± SEM of $n = 3$ cells for WT and $n = 5$ cells for R4H) WT: 1.27 ± 0.64; R4H: 0.96 ± 0.24.

time constants ($\tau_{R(fast)}$ / $\tau_{R(slow)}$ in ms) were for WT: 15.5 ± 22.1 / 60.6 ± 91.8 (−80 mV); 7.3 ± 2.2 / 42.4 ± 68.7 (−100 mV); 3.1 ± 0.9 / 26.5 ± 48.3 (−120 mV) and for R3/4/5H: 7.6 ± 4.8 / 55.3 ± 25.2 (−80 mV); 6.7 ± 2.2 / 41.0 ± 26.8 (−100 mV); 3.8 ± 1.1 / 27.0 ± 21.4 (−120 mV). Thus, only at −80 mV the recovery kinetics of WT was moderately delayed and less complete compared to R3/4/5H, which was most probably caused by the predominating slow-mode channels of WT. In comparison to our previously studied mutation R1635H (R4H), which drastically slows the recovery from fast inactivation (examples shown in Fig. 5*A*), the triple mutation R3/4/5H recovers similarly to WT, as also observed for the double mutation R4/5H (Kühn & Greeff, 1999).

Modification by Site-3 Toxins (ATX-II)

Site-3 toxins have been shown to selectively impair the movement of voltage sensor S4D4 (Sheets & Hanck, 1995). Moreover, Sheets et al. (1999) demonstrated that the replacement of each of the three outermost arginines of voltage sensor S4D4 does not change the strong impact of these toxins on the inactivation time course as observed in WT, suggesting that the toxin effect surpasses the impact of the individual mutations. This result supports the conclusions of Sheets et al. (2000) that the movement of voltage sensor S4D4 is actually inhibited by site-3 toxins, at least during the early phase of inactivation. In line with these data is our finding that in the presence of 2 μM ATX-II, the very slow recovery kinetics of R4H (Fig. 5*A*, *see* also Kühn & Greeff, 1999) became as fast as the corresponding WT recovery (Fig. 5*B*). Thus, the impact of site-3 toxins seems to be independent from the previously changed kinetics of the mutated voltage sensor S4D4.

However, the comparison of the macroscopic current decay of I_{Na} recorded from WT and R3/4/5H in the presence of 2 μM ATX-II (Fig. 6*A*) reveals that for R3/4/5H the toxin exerted only minor effects on the fast inactivation kinetics, whereas WT displays the characteristically slowed inactivation time course and a substantial plateau current as already described by others (e.g., Benzinger, Tonkovich & Hanck, 1999). The corresponding time constants given in Table 2 demonstrate that both gating modes of WT were profoundly slowed by ATX-II, whereas in R3/4/5H, both time constants were even slightly decreased in the presence of the toxin. Also included in Table 2 are the corresponding activation time constants (τ_m) that were determined as described in the legends of Figs. 2*A* and 8*C*. The data show that in particular for WT, the activation time constants were markedly reduced in the presence of ATX-II. In contrast, the τ_m - values of R3/4/5H were only minimally affected by the toxin.

On the other hand, the comparison of Figs. 4*A* and 6*B* demonstrates that the recovery kinetics of R3/4/5H was accelerated by ATX-II but to a significantly smaller extent than observed in WT or R1635H (Fig. 5).

The reduced impact of ATX-II on the time course of fast inactivation and recovery of R3/4/5H

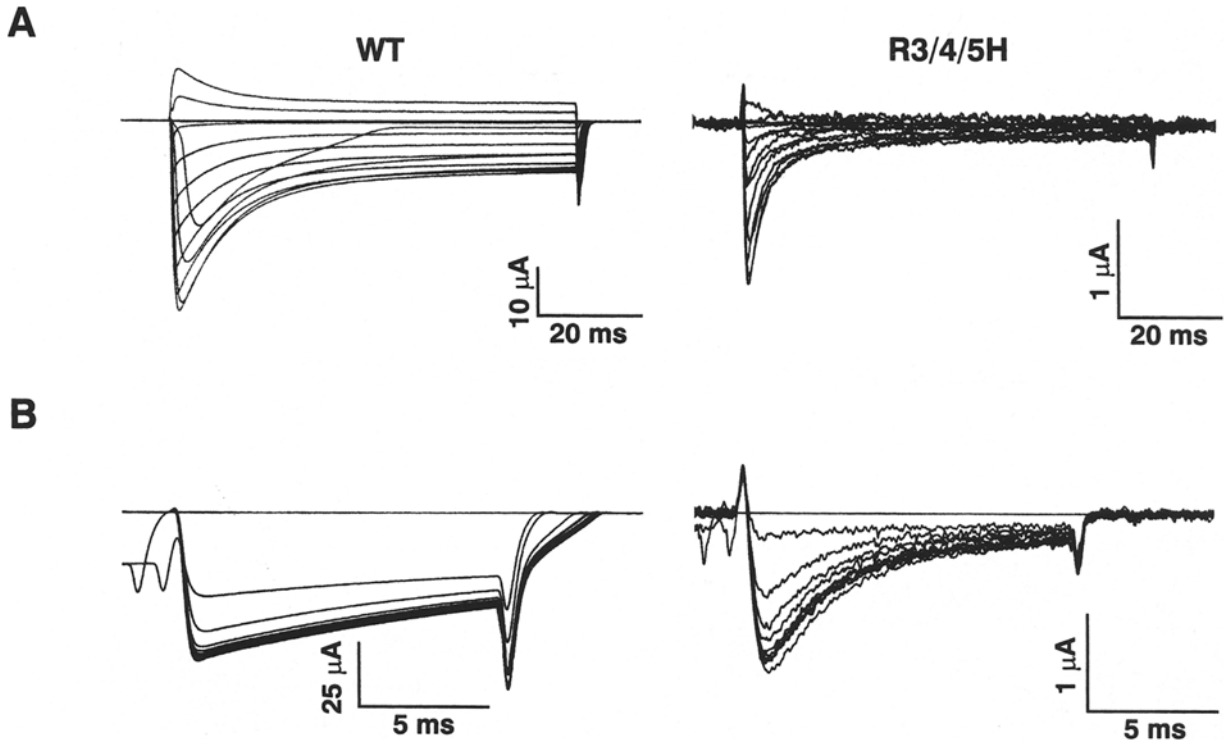

Fig. 6. Effect of ATX-II on the inactivation kinetics of WT and R3/4/5H. (*A*) Typical sodium current families recorded in the presence of 2 μM ATX-II (for comparison *see* Fig. 1*A*). Currents were elicited by depolarizing pulses from −80 mV to +80 mV from a holding potential of −100 mV; test pulse duration 80 ms. For the comparison of the effects on the time constants of activation and inactivation induced by the toxin, *see* Table 2. (*B*) Recovery from fast inactivation of WT and R3/4/5H performed at a recovery potential of −100 mV, as described in the legend of Fig. 4 (for comparison, *see* also Fig. 4*A*). Note the different impact of the toxin on the fast inactivation kinetics as well as on the recovery kinetics of WT and R3/4/5H.

Table 2. Time constants of I_{Na} decay of WT and R3/4/5H obtained at 0 mV in the absence or in the presence of ATX

	WT (MBS)	WT (ATX)	R3/4/5H (MBS)	R3/4/5H (ATX)
τ_m	0.89 ± 0.3	0.29 ± 0.04	0.71 ± 0.2	0.51 ± 0.1
$\tau_{h(fast)}$	0.86 ± 0.4	8.55 ± 1.6	3.70 ± 0.7	2.62 ± 0.4
$\tau_{h(slow)}$	11.8 ± 4.8	55.1 ± 24.7	19.1 ± 1.1	16.0 ± 2.0

The data (mean in ms ± SD of n = 3–6 cells) were obtained as described in the legends of Figs. 2 and 8. ATX was used at a concentration of 2 μM. Recordings were performed at 15°C.

could also reflect a decreased toxin affinity of the mutant although the putative binding site of site-3 toxins was localized in the S3–S4 extracellular loop of domain 4 (Rogers et al., 1996). Therefore, we examined the toxin binding in concentration experiments of ATX-II; the inactivation kinetics was studied in WT and in R3/4/5H at five different toxin concentrations, and further in the absence (Fig. 7*A*) or in the presence (Fig. 7*B*) of the β_1 subunit. The results obtained and fitted to a single-ligand-to-receptor curve show that the affinity of rat brain IIA sodium channels to ATX-II was largely unaffected by the mutation R3/4/5H (Fig. 7*C*) with an EC_{50} of between 0.2 to 0.4 μM ATX-II. Likewise, the coexpression of the β_1 subunit did not significantly change the effect of ATX-II on sodium channel gating. Thus, only the intrinsic effect of the toxin (the size of the plateau current relative to the peak) was markedly reduced in R3/4/5H, most probably due to a changed mobility of S4D4, which is in agreement with our other data of this mutant (*see* below).

Analysis of the Gating Kinetics at Low Temperature

The slowed inactivation time course as well as the reduced impact of ATX-II on R3/4/5H suggest that the mobility of voltage sensor S4D4 is markedly changed in the mutant. Correspondingly, in case of an involvement of S4D4 in channel activation, R3/4/5H should also display different activation kinetics, if compared to WT. In order to get some information

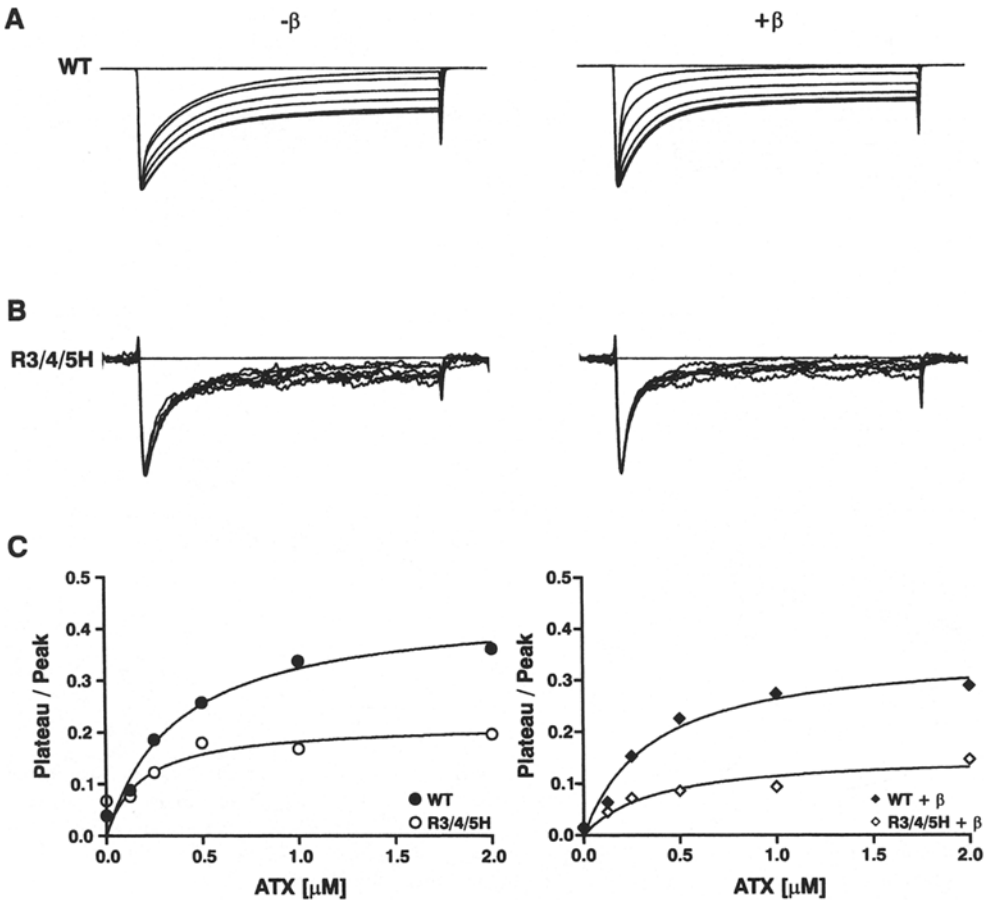

Fig. 7. Concentration-dependent effect of ATX-II on ratio of plateau to peak sodium currents. (*A–C*) Effect of ATX-II at bath concentrations of 0, 0.13, 0.25, 0.5, 1.0, and 2.0 μM on macroscopic sodium currents of WT and R3/4/5H obtained from single-cell experiments without (*A*) or with (*B*) β_1 coexpression. Depolarizing pulses were to 0 mV from a holding potential of −100 mV, test pulse duration 80 ms. Traces were normalized to peak. (*C*) Ratios of plateau currents to peak currents obtained from *A* and *B* were plotted against toxin concentration. Note that the maximal effect of ATX-II was reached at concentrations of about 2 μM both in WT and R3/4/5H. The single-ligand binding was checked graphically in a Lineweaver-Burke-plot where the data points are close to a straight line (compare Denac et al., 2002). Accordingly, the data were fitted to a single-ligand-to-receptor binding curve: $y = y_{max} \cdot x/(EC_{50} + x)$. EC_{50ATX} in μM was for WT 0.4 ($-\beta_1$) and 0.4 ($+\beta_1$), and for R3/4/5H 0.2 ($-\beta_1$) and 0.4 ($+\beta_1$); y_{max} in % was for WT 45 ($-\beta_1$) and 36 ($+\beta_1$), and for R3/4/5H 22 ($-\beta_1$) and 16($+\beta_1$).

about the very fast activation kinetics of WT and mutant rBIIA sodium channels, we recorded at a bath temperature of 8°C where the channel kinetics is relatively slow compared to the capacitance transient, which reflects the speed of voltage control. Figure 8 shows normalized current traces of WT and R3/4/5H superimposed and recorded at 15°C (*A*) and 8°C (*B*), respectively. The currents were elicited by step depolarization of 80 ms duration to the indicated voltages ranging between −20 mV and +20 mV from a holding potential of −100 mV. First of all, the comparison demonstrates that the inactivation kinetics of R3/4/5H was twice more sensitive to low temperature than observed in WT (*see* corresponding time constants included in Table 1). These data suggest that, especially in R3/4/5H, the mobility of S4D4 was affected by low temperature.

Next, we determined both the half times to activation ($t_{1/2}$) and the activation time constants (τ_m) of WT and R3/4/5H from single current traces recorded at 8°C under optimized clamping conditions in a 20 ms time window and with a resolution of 20 μs per data point (*see* sample traces in inset of Figure 8*B*). The activation time constant (τ_m) and two inactivation time constants ($\tau_{h(fast)}/\tau_{h(slow)}$, *see* legend) were derived. It is clearly seen that the activation kinetics of R3/4/5H was not significantly different from WT if one takes further into account that the two independent characteristic parameters of activation, τ_m and $t_{1/2}$, yielded slightly opposing but close to WT data and, in addition, that the about 5-fold slowed inactivation time course of the mutant certainly affects the measurement of the corresponding activation kinetics (Fig. 8*C*; *see* also Discussion).

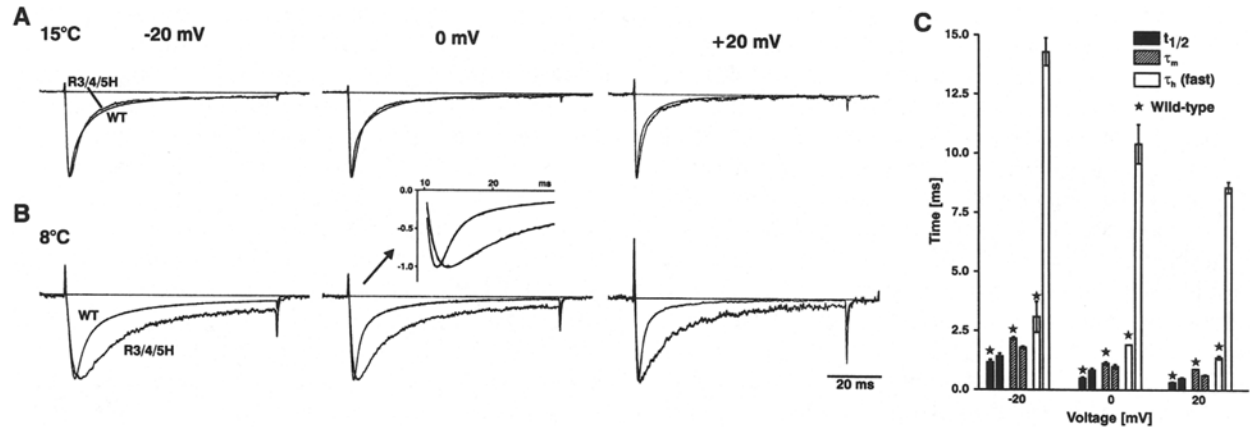

Fig. 8. Activation and inactivation kinetics of WT and R3/4/5H at low temperature. (*A–B*) Comparison of typical single-current traces of WT and R3/4/5H recorded at 15°C (*A*) or 8°C (*B*). Currents were elicited by depolarizing pulses of 80 ms duration to the indicated voltages from a holding potential of −100 mV. Traces were normalized to peak. The data were fitted to a triple-exponential curve $Y = (1 - \exp(-t/\tau_m))^3 \cdot [A1 \cdot \exp(-t/\tau_{h1}) + A2 \cdot \exp(-t/\tau_{h2}) + A3]$ with activation time constant (τ_m) and inactivation time constants ($\tau_{h(fast)}$/ $\tau_{h(slow)}$ as also shown in Table 1). An example of data and fit is demonstrated in the inset for 0 mV at 8°C with τ_m in ms for WT/R3/4/5H equal to 1.01/1.07 and $\tau_{h,(fast)}$ in ms equal to 1.99/9.55. (*C*) Effects of mutation R3/4/5H on time constants of half activation ($t_{1/2}$), activation (τ_m) and fast inactivation ($\tau_{h(fast)}$) obtained at 8°C (*compare* inset in *B*), with minimal R_s-distortion and at constant clamping speed. The corresponding WT values are indicated by asterisks. The values for $t_{1/2}$ in ms (mean ± SD obtained at −20 mV / 0 mV / +20 mV for n = 3 cells) were WT: 1.16 ± 0.2 / 0.49 ± 0.1 / 0.31 ± 0.1 and R3/4/5H: 1.41 ± 0.2/0.83 ± 0.1 / 0.48 ± 0.1) and for τ_m in ms (mean ± SD obtained at −20 mV/0 mV/+20 mV for n = 2 cells) were WT: 2.16 ± 0.1/1.13 ± 0.1/0.89 ± 0.01 and R3/4/5H: 1.78 ± 0.1/0.99 ± 0.1/0.63 ± 0.05).

Discussion

In continuation of our former approach to inhibit the movement of S4D4 by the systematic replacement of central arginines to histidines in this voltage sensor (Kühn & Greeff, 1999), we introduced the triple mutation R1632H + R1635H + R1638H (= R3/4/5H) and analyzed the effects on the gating kinetics of rat brain IIA sodium channel. First of all, the mutant showed a considerably reduced expression compared to WT. This was reflected both on the level of the ionic current as well as of the gating current, the latter being too small to be separated from baseline noise and asymmetry artifacts, respectively. The presence of inadvertent mutations in other regions of the channel could be excluded because several clones were tested yielding the same results. Likewise, a specific reduction of the available gating charge of R3/4/5H due to the inhibition of the mobility of S4D4, as observed by Sheets et al. (1995; 1999; 2000) in the presence of site-3 toxins, is rather unlikely because the well-resolved sodium current of R3/4/5H displayed quite normal activation and inactivation properties. Instead, it is conceivable that the triple mutation in some way interferes with the proper folding of the protein because the substituted arginines possibly participate in a network of charged residues that stabilizes the channel structure. Similar results were described for some mutants of S4 segments of voltage-dependent sodium channels (Stühmer et al., 1989) or potassium channels (Papazian et al., 1995), but these mutations caused the loss of functional expression altogether. In other studies performed in our own lab we noticed that some sodium channel mutants also showed decreased expression levels, if compared to WT (e.g., *Paramyotonia congenita* equivalent mutation R1626C or IFM1488-1490QQQ; *unpublished data*). There, we have some experimental data that these channels, which show strongly reduced or completely abolished fast inactivation properties, were leaky for sodium during expression in *Xenopus* oocytes and, therefore, indirectly reduce the expression level (Greeff & Kühn, 2000).

In a previous study we have demonstrated that the replacements of arginines by histidines in the central part of voltage sensor S4D4 (mutation R4H, R4/5H and R5H) predominantly induce steric effects rather than changing the voltage dependence of the channel (Kühn & Greeff, 1999). Accordingly, the slight decrease of the voltage dependence for entry and exit from the inactivated state observed in R3/4/5H suggests that the substitution of the third arginine is responsible for this additional effect. This conclusion is supported by the data of other groups (Chen et al., 1996; Yang et al., 1996; Sheets et al., 1999). As to the charge, Histidine has, depending on the local protein environment, a pK of 5.6–7.0 and therefore, the charge of this amino acid could change under varying pH conditions (Sancho et al., 1992). Despite the fact, that there was no control of the intracellular solution using the two-electrode voltage-clamp technique, we varied the extracellular pH between 5 and 9 without seeing any effects (*data not shown*).

As established by the authors (Kühn & Greeff, 1999), the mutation R1635H (R4H) in the central part of S4D4 dramatically increased (~20-fold) the recovery time constants of both fast inactivation and voltage-sensor immobilization (visible in the gating current) and therefore, exerted one of the strongest effects on the kinetics of S4D4 compared to previously described mutations of this voltage sensor (Chahine et al., 1994; Chen et al., 1996; Kontis & Goldin, 1997). In contrast to recovery, R4H showed only a small deceleration of the kinetics of current decay compared to WT. On the other hand, the double mutation R1635H + R1638H (R4/5H) analyzed in the same study, moderately (~2-fold) slowed the recovery kinetics but increased the time constants of fast inactivation to a larger extent than observed in R4H. Similarly, the mutation R3/4/5H significantly slowed the time course of fast inactivation, whereas the recovery kinetics was almost identical to WT. These results suggest that a single histidine-for-arginine substitution in the central part of S4D4 is less tolerable for the recovery from fast inactivation, and vice versa less critical for the development of fast inactivation, than the corresponding double or triple substitution. In line with this observation are the data of Groome et al. (2002) who found that different alterations of the structure of the arginine moiety at either R4 or R5 impedes or facilitates the movement of voltage sensor S4D4 during deactivation.

The bimodal gating behavior characteristic for WT rBIIA sodium channels, if expressed in *Xenopus* oocytes without the accessory β_1 subunit, is less pronounced in R3/4/5H, which is reflected by the monophasic recovery time course of the mutant. Accordingly, the pronounced shift to the fast gating mode induced by β_1 coexpression is not observed in R3/4/5H. This result suggests a putative role of S4D4 for the determination of the gating mode during expression of rat brain sodium channels in *Xenopus* oocytes. Accordingly, recent findings of Mantegazza et al. (2001) had demonstrated the principal role of the C-terminal domain of brain and cardiac sodium channels for the kinetics and voltage dependence of inactivation.

Apart from single or multiple arginine substitutions also site-3 toxins selectively change the mobility of voltage sensor S4D4 (Sheets et al., 1995; 1999; 2000; Benzinger et al., 1999). Furthermore, Sheets et al. (1999) demonstrated that the replacement of the three outermost arginines of S4D4 did not change the effect of site-3 toxin on the fast inactivation kinetics although each of these mutations alone markedly slowed the inactivation time course of the channel. In line with this observation is our finding that the 20-fold slowed recovery time courses of mutant R4H became as fast as the corresponding WT recovery in the presence of ATX-II. Hence, the impact induced by the toxin was independent of the corresponding effect of the mutations. These data support the hypothesis of Sheets et al. (2000) that site-3 toxins selectively inhibit the movement of voltage sensor S4D4. However, a remaining question is the extent of this inhibition. If site-3 toxins actually arrest the movement of S4D4, this should abolish fast inactivation because a series of experimental data have clearly demonstrated the principal role of this voltage sensor in sodium channel fast inactivation (Chahine et al., 1994; Yang & Horn, 1995; Chen et al., 1996; Yang et al., 1996; Kontis & Goldin, 1997; Kühn & Greeff, 1999). Moreover, if the movement of S4D4 is in some way coupled to the activation process, which is suggested by the data of Horn et al. (2000), then channel activation should be prevented or at least severely impaired by the toxin, which is obviously not the case.

In fact, we found that the impact of ATX-II on the fast inactivation kinetics of R3/4/5H was considerably reduced compared to WT. To our knowledge, this is the first mutation in a region other than the putative binding site that reduces the efficacy of ATX-II without changing significantly the affinity of the channel for the toxin. According to our hypothesis, the effect of ATX-II can be explained by electrostatic interactions of the positively charged toxin with the outermost arginines of S4D4. As a result, the outward movement of S4D4 is delayed leading to slowed inactivation kinetics and vice versa the return of the voltage sensor is favored, implicating an accelerated recovery from fast inactivation. Therefore, the data of the current study demonstrate that the mobility of S4D4 was considerably changed by the mutation R3/4/5H, which was reflected by the slowed inactivation kinetics and the reduced impact of ATX-II.

While this study has clearly confirmed the well-established hypothesis that the voltage sensor S4D4 is involved in fast inactivation, it shall now be discussed what bearing our data have for a role of this segment for activation. Recalling the finding that R3 moves through the "gating pore", as shown by cysteine mutagenesis and MTSET accessibility experiments (Yang et al., 1996), it would appear that a replacement by the bulky histidine would hinder the outward movement of S4D4 through the "gating pore" at an earlier stage than R4H or R5H. According to our previous study, R4H and R5H have only an impact on fast inactivation but not on activation (Kühn & Greeff, 1999). We then concluded that at least one voltage-dependent conformational step controls the inactivation gate. However, this did not exclude a first step of outward movement of S4D4 that might control an activation gate or might delay inactivation. For the extended mutation R3/4/5H it appears plausible that it would block the outward movement at an earlier stage and would more likely indicate a putative involvement of S4D4 in activation.

To analyze a putative impact on activation, the experiments obtained at the lower temperature of 8°C were used where the fast sodium channel currents are slow in comparison to the speed of the clamp. Furthermore, we used an optimized two-electrode voltage clamp that allowed us to establish fast voltage steps at the whole oocyte (Greeff & Polder, 1998). This clamp design had already proved its worth for the recording of the very fast sodium channel gating currents (Kühn & Greeff, 1999; Greeff & Kühn, 2000). Special care was taken to adjust the R_s compensation such that the speed-limiting capacitance transient was fast and of equal speed in WT and mutant channel-expressing oocytes. R_s errors were further reduced by choosing oocytes with small sodium currents, especially WT. For the analysis, currents were recorded in 100 and 20 ms time windows to allow fitting of both, the inactivation and the activation phase (Fig. 8*B* and 8*C*). While $\tau_{h(fast)}$ is increased by a factor of 4 to 5, activation is hardly changed in R3/4/5H compared to WT. The data also show that the fast inactivation kinetics of R3/4/5H at 8 °C was slowed to a clearly larger extent than observed in WT, which might suggest that the movement of the mutated S4D4 segment was reduced by sterical obstruction. As a regular feature it is observed that the time to half activation $t_{1/2}$ is about 20% larger in the mutant, while the fitted τ_m is about 20% smaller than in WT. The fitted equation is of the Hodgkin-Huxley type with parallel activation and inactivation, i.e., a product of a rising and a declining exponential. For such systems it is easily shown that the apparent $t_{1/2}$ becomes larger for a constant τ_m but increasing $\tau_{h\ (fast)}$. It is further easily seen that the open-probability P^o at peak ionic current gets larger for slower inactivation and constant τ_m; slow inactivation allows more channels to be open before they inactivate. In our data, the WT P^o is between 0.3 and 0.5 while it is about 0.8 for the mutant, as obtained by the fitting. This has two consequences for the interpretation of our data: (i) The I/V curves (Fig. 1*B*), which usually show peak ionic currents and not the fraction of activated channels, should be corrected for inactivation. Then, the small difference, being anyway partly due to some R_s error for WT would become even less significant; however, a correction for inactivation can only properly be done if the coupling mode of activation to inactivation is known, which is presently not the case. (ii) The other consequence is that the time course of the sodium current traces should not be compared with peaks normalized, but the peak for the mutant should be larger according to the larger P^o and then the initial time course becomes as fast as in WT or even faster, depending on the model one uses to correct for inactivation.

In summary, we conclude that activation is not slowed in R3/4/5H and, therefore, the data of this study still give no support for an involvement of S4D4 as voltage sensor for an activation gate. However, this question is still not fully settled and our data have to be seen as experimental evidence to be compared with other data that support a first activation step (Horn et al., 2000) or do not support it (Sheets et al., 2000); also data about S4D4 obtained by a new experimental approach conform with both (Chanda & Bezanilla, 2002). Finally, it has to be mentioned that our study has dealt with the clear-cut effects on fast inactivation. Other studies suggest an additional role of the S4D4 mid-region arginines (Mitrovic, George and Horn, 2000) or the P-loop region of domain 4 (Hilber et al., 2002) for the so-called slow inactivation. Such slow inactivation was not addressed in the study reported here, and therefore, we exclusively used pulse protocols where slow inactivation effects were negligible.

We thank Dr. Alan L. Goldin (Irvine, CA) for providing the cDNA of the wild-type rat brain IIA sodium channel (pVA2580) and the high expression vector (pBSTA). We are grateful to Dr. William A. Catterall (Seattle, WA) for providing the cDNA of the β_1-subunit, to Rainer Polder (npi electronic GmbH, Tamm, Germany) for his support in developing the modified two-electrode voltage clamp and to Christian Gasser (Zürich, Switzerland) for his graphical assistance. The work was supported by the Swiss National Science Foundation (grant No. 31-37987.93) and the Hartmann-Müller-Stiftung.

References

Balser, J.R., Nuss, H.B., Chiamvimonvat, N., Pérez-García, M.T., Marbán, E., Tomaselli, G.F. 1996. External pore residue mediates slow inactivation in μl rat skeletal muscle sodium channels. *J. Physiol.* **494:**431–442

Bennett, P.B., Makita, N., George, A.L., Jr. 1993. A molecular basis for gating mode transitions in human skeletal muscle sodium channels. *FEBS Lett.* **326:**21–24

Benzinger, G.R., Tonkovich, G.S., Hanck, D.A. 1999. Augmentation of recovery from inactivation by site-3 Na channel toxins. *J. Gen. Physiol.* **113:**333–346

Catterall, W.A. 1986. Molecular properties of voltage-sensitive sodium channels. *Ann. Rev. Biochem.* **55:**953–985

Cha, A., Ruben, P.C., George, A.L., Jr., Fujimoto, E., Bezanilla, F. 1999. Voltage sensors in domains III and IV, but not I and II are immobilized by Na^+ channel fast inactivation. *Neuron.* **22:**73–87

Chahine, M., George, A.L., Jr., Zhou, M., Ji, S., Sun, W., Barchi, R.L., Horn, R. 1994. Sodium channel mutations in paramyotonia congenita uncouple inactivation from activation. *Neuron.* **12:**281–294

Chanda, B., Bezanilla, F. 2002. Tracking voltage-dependent conformational changes in skeletal muscle sodium channel during activation. *J. Gen. Physiol.* **120:**629–645

Chen, L.-Q., Santarelli, V., Horn, R., Kallen, R.G. 1996. A unique role for the S4 segment of domain 4 in the inactivation of sodium channels. *J. Gen. Physiol.* **108:**549–556

Denac, H., Mevissen, M., Kühn, F.J.P., Kühn, C., Guionaud, C.T., Scholtysik, G., Greeff, N.G. 2002. Molecular cloning and functional characterization of a unique mammalian cardiac

Na(v) channel isoform with low sensitivity to the synthetic inactivation inhibitor (-)-(S)-6-amino-alpha-[(4-diphenylmethyl-l-piperazinyl)-methyl]-9H-purine-9-ethanol (SDZ 211-939). *J. Pharm. Exptl. Ther.* **303:**89–98

Greeff, N.G., Kühn, F.J.P. 2000. Variable ratio of permeability to gating charge of rBIIA sodium channels and sodium influx in *Xenopus* oocytes. *Biophys. J.* **79:**2434–2453

Greeff, N.G., Polder, R. 1998. Optimization of a two-electrode voltage clamp for recording of sodium ionic and gating currents from *Xenopus* oocytes. *Biophys. J.* **74:**A402

Groome, J., Fujimoto, E., Walter, L., Ruben, P.C. 2002. Outer and central charged residues in DIVS4 of skeletal muscle sodium channel have differing roles in deactivation. *Biophys. J.* **82:**1293–1307

Hilber, K., Sandtner, W., Kudlacek, O., Schreiner, B., Glaaser, I., Schuetz, W., Fozzard, H.A., Dudley, S.C., Todt, H. 2002. Interaction between fast and ultra-slow inactivation in the voltage-gated sodium channel: Does the inactivation gate stabilize the channel structure? *J. Biol. Chem.* **277:**37105–37115

Horn, R., Shinghua, D., Gruber, H.J. 2000. Immobilizing the moving parts of voltage-gated ion channels. *J. Gen. Physiol.* **116:**461–475

Isom, L.L., De Jongh, K.S., Catterall, W.A. 1994. Auxiliary subunits of voltage-gated ion channels. *Neuron.* **12:**1183–1194

Isom, L.L., De Jongh, K.S., Patton, D.E., Reber, B.F.X., Offord, J., Charbonneau, H., Walsh, K., Goldin, A.L., Catterall, W.A. 1992. Functional coexpression of the β-1 subunit of the rat brain sodium channel. *Science.* **256:**839–842

Ji, S., George, A.L., Jr., Horn, R., Barchi, R.L. 1994. Voltage-dependent regulation of modal gating in the rat SkM1 sodium channel expressed in *Xenopus* oocytes. *J. Gen. Physiol.* **104:**625–643

Kontis, K.J., Goldin, A. 1997. Sodium channel inactivation is altered by substitution of voltage sensor positive charges. *J. Gen. Physiol.* **110:**403–413

Kontis, K.J., Rounaghi, A., Goldin, A. 1997. Sodium channel activation gating is affected by substitutions of voltage sensor positive charges in all four domains. *J. Gen. Physiol.* **110:**391–401

Kühn, F.J.P., Greeff, N.G. 1999. Movement of voltage sensor S4 in domain 4 is tightly coupled to sodium channel fast inactivation and gating charge immobilization. *J. Gen. Physiol.* **114:**167–183

Kühn, F.J.P., Greeff, N.G. 2002. Mutation D384N alters recovery of the immobilized gating charge in rat brain IIA sodium channels. *J. Membrane Biol.* **185:**145–155

Mantegazza, M., Yu, F.H., Catterall, W.A., Scheuer, T. 2001. Role of the C-terminal domain in inactivation of brain and cardiac sodium channels. *Proc. Natl. Acad. Sci. USA* **98:**15348–15353

Mitrovic, N., George, A.L., Jr., Horn, R. 2000. Role of domain 4 in sodium channel slow inactivation. *J. Gen. Physiol.* **115:**707–718

Moorman, J.R., Kirsch, G.E., VanDongen, A.M.J., Joho, R.H., Brown, A.M. 1990. Fast and slow gating of sodium channels encoded by a single mRNA. 1990. *Neuron.* **4:**243–252

Moran, O., Melani, R., Nizzari, M., Conti, F. 1998. Fast- and slow-gating modes of the sodium channel are altered by a paramyotonia congenita-linked mutation. *J. Bioenerg. Biomembr.* **30:**579–588

Noda, M., Ikeda, T., Suzuki, H., Takeshima, H., Takahashi, H., Kuno, M., Numa, S. 1986. Expression of functional sodium channels from cloned cDNA. *Nature.* **322:**826–828

Papazian, D.M., Shao, X.M., Seoh, S-A., Mock, A.F., Huang, Y., Wainstock, D.H. 1995. Electrostatic interactions of S4 voltage sensor in *Shaker* K^+ channel. *Neuron.* **14:**1293–1301

Patton, D.E., Isom, L.L., Catterall, W.A., Goldin, A.L. 1994. The adult rat brain β_1 subunit modifies activation and inactivation gating of multiple sodium channel α subunits. *J. Biol. Chem.* **269:**17649–17655

Rogers, J.C., Qu, Y., Tanada, T.N., Scheuer, T., Catterall, W.A. 1996. Molecular determinants of high affinity binding of α-Scorpion Toxin and Sea Anemone Toxin in the S3-S4 extracellular loop in domain IV of the Na^+ channel α subunit. *J. Biol. Chem.* **271:**15950–15962

Sancho, J., Serrano, L., Fersht, A.R. 1992. Histidine residues at the N- and C-termini of alpha-helices: perturbed pKas and protein stability. *Biochemistry.* **31:**2253–2258

Schreibmayer, W., Lester, H.A., Dascal, N. 1994. Voltage clamping of *Xenopus laevis* oocytes utilizing agarose-cushion electrodes. *Pfluegers Arch.* **426:**453–458

Sheets, M.F., Hanck, D.A. 1995. Voltage-dependent open-state inactivation of cardiac sodium channels: gating current studies with Anthopleurin-A toxin. *J. Gen. Physiol.* **106:**617–640

Sheets, M.F., Kyle, J.W., Kallen, R.G., Hanck, D.A. 1999. The Na channel voltage sensor associated with inactivation is localized to the external charged residues of domain IV, S4. *Biophys. J.* **77:**747–757

Sheets, M.F., Kyle, J.W., Hanck, D.A. 2000. The role of the putative inactivation lid in sodium channel gating current immobilization. *J. Gen. Physiol.* **115:**609–619

Shih, T.M., Smith, R.D., Toro, L., Goldin, A.L. 1998. High-level expression and detection of ion channels in *Xenopus* oocytes. *Meth. Enzymol.* **293:**529–556

Sigworth, F.J. 1993. Voltage gating of ion channels. *Q. Rev. Biophys.* **27:**1–40

Stühmer, W., Conti, F., Suzuki, H., Wang, X., Noda, M., Yahagi, N., Kubo, H., Numa, S. 1989. Structural parts involved in activation and inactivation of the sodium channel. *Nature.* **339:**597–603

Yang, N., Horn, R. 1995. Evidence for voltage dependent S4 movements in sodium channels. *Neuron.* **15:**213–218

Yang, N., George, A.L., Horn, R. 1996. Molecular basis of charge movement in voltage-gated sodium channels. *Neuron.* **16:**113–122

Yellen, G. 1998. The moving parts of voltage-gated ion channels. *Q. Rev. Biophys.* **31:**239–295

Zhou, J., Potts, J.F., Trimmer, J.S., Agnew, W.S., Sigworth, F.J. 1991. Multiple gating modes and the effect of modulating factors on the μl sodium channel. *Neuron.* **7:**775–785